

Figure 2. Isotherm (curve a) and surface potential (curve b). Inset is a plot of $\Delta\Delta V$ versus molecular area.

solution. Data have been taken at room temperature. The trough is set in an enclosure so that it is protected from dust and drafts.

Surface potential has been measured at the air–water interface between a gilded vibrating electrode and a platinum counter electrode immersed below the water surface.

Brewster angle microscopy¹⁷ (BAM) observations have been performed with an apparatus from NFT (Göttingen, Germany, www.nanofilm.de). The observations are made at Brewster angle (around 53.15° for an air–water interface) incidence; hence the limited depth of focus of the objective makes it impossible to have an entirely sharp picture.¹⁸ When the film under study is motionless, it is possible to scan the entire field while adjusting the film–objective distance. Unfortunately, the films presented here are quite mobile, so each picture is taken as one snapshot. Consequently, the focus is more and more out when going from the center of a picture to the upper and lower edges; this effect is clearly visible on some pictures. Each picture encompasses a field of 500 $\mu\text{m} \times 400 \mu\text{m}$, unless otherwise specified.

III. Results and Discussion

Although not amphiphilic in the traditional sense,¹⁹ the compound has proven able to form organized films at the air–water interface. Therefore, the first question that comes to mind is which end of the molecule plays the hydrophilic role? The sulfinate group is strongly hydrophilic, but having this part of the molecule in contact with the water would mean having the C₁₀ alkane chain also in water. This is not necessarily a problem as short alkane chains are slightly soluble in water, but we believe that the siloxane group actually acts as the hydrophilic head. At least two observations can justify this assumption: first, pure poly(dimethylsiloxane) forms Langmuir films²⁰ while pure alkanes do not and, second, Ibn-Elhaj et al. have observed on a similar compound (their molecule has the siloxane part attached next to the sulfinate group) that removing the siloxane moiety precludes formation of any Langmuir film,²¹ suggesting that the siloxane indeed acts as a polar head. It is true that, with another compound possessing a siloxane group, Ibn-Elhaj et al. have brought evidence that the siloxane group could be away from the air–water interface,²² but in this case their molecule also bore a strongly polar cyano group which made a much better hydrophilic head.

The surface pressure π as a function of molecular area A is given in Figure 2, curve a. Surface pressure starts to rise at $A \approx 150 \text{ Å}^2$ (point A on the curve). Such a large molecular area indicates that the molecules must initially lie flat on the water surface. Authors of ref 21, with a very similar molecule, observe a comparably large molecular area and also conclude that the molecules lie parallel to the water surface. Below point A the surface pressure then steadily increases until $A \approx 113 \text{ Å}^2$ (point B on the curve), when compressibility suddenly becomes very

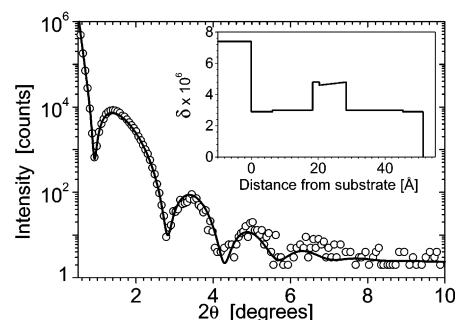


Figure 3. X-ray diffraction structure of a film in the bilayer regime deposited on silicon. Solid line is the fit to the data points. Inset is the variation of δ as a function of the distance from the silicon substrate, as resulting from the fit.

high. At point B, a first-order transition takes place. It corresponds to the nucleation of a new layer that continues to grow all along the plateau region of $100 \text{ Å}^2 \geq A \geq 40 \text{ Å}^2$ molecular areas, as BAM observations confirm (see below). At $A \approx 32 \text{ Å}^2$ (point C) the surface pressure then increases again but levels off (point D) after only a small jump of pressure $\Delta\pi \approx 5 \text{ mN} \cdot \text{m}^{-1}$. Here again Brewster angle microscopy confirms that this plateau corresponds to the nucleation of a new layer (see below). Unfortunately, the compression ratio of our trough is insufficient to fully explore all the features of the isotherm and only the beginning of this second plateau can be seen in Figure 3. Within the accuracy of our measurements, the isotherms are perfectly reversible in the sense that the π – A point representing the status of the film on the isotherm always moves along the same curve with absolutely no hysteresis, regardless of the values of π and A , which is rather unusual. This means that the films are always really in the isothermal regime, at least up to the maximum compression speed used here, ca. $10 \text{ Å}^2 \cdot \text{molecule}^{-1} \cdot \text{min}^{-1}$, and that the molecules have little or no tendency to stick together with irreversible interactions (no entanglements or H-bonds). A similar behavior, i.e., layering transitions and little hysteresis, has been reported in Langmuir films of smectogen molecules,²² with however the difference that the second and third layers were actually bilayers²³ instead of being only one molecule thick in our case. In both cases the molecule possesses a siloxane segment connected via a short paraffinic chain to the rigid core of the molecule. It is therefore reasonable to make this particular structure responsible for the exceptional reversibility of the compression isotherms.

The building up of the films is indeed a complex process with various changes occurring almost simultaneously. As noted above, the formation of the first layer probably begins with the molecules being more or less parallel to the surface. This configuration is certainly favored by the aforementioned dipoles which must tend to point toward the water and the hydrophilic nature of the sulfinate moiety. As compression progresses, one end could lift up and the molecular long axis would go closer to the vertical, as is usually observed with molecules having two hydrophilic groups.²⁴ Should this process occur between points A and B, the molecular tilt angle would then go from $\sim 79^\circ$ at point A to $\sim 75^\circ$ at point B, as estimated from the values of the molecular volume and molecular areas. Nevertheless, we may not discard the possibility that the molecules stay parallel to the interface and that the film only undergoes intramolecular conformational changes. This hypothesis could be supported by the large value of the molecular area at point B, about 4 times larger than the estimated cross section of one molecule ($\sim 30 \text{ Å}^2$ on average, $\sim 45 \text{ Å}^2$ for the siloxane moiety). After that, some molecules get expelled from this first homogeneous layer

and a second layer nucleates atop the first one. If the area per molecule were identical in all layers, the molecular areas at points B and D would be in the 1:0.5 proportion²⁵ when we observe 1:0.25. This implies that the internal structures of the first and second layers are very different, as will be seen below.

Measurement of the surface potential ΔV has also been recorded during the compression of the film, and the corresponding curve is given in Figure 2, curve b. Surface potential increases rapidly between $A \approx 156 \text{ \AA}^2$ and $A \approx 146 \text{ \AA}^2$, where it reaches a value of 0.32 V. At this point the first monolayer is complete (i.e., no holes) and starts to be compressed. During compression of the monolayer, ΔV rises slowly to its peak value of 0.38 V, reached for $A \approx 113 \text{ \AA}^2$. During the nucleation of the second layer, ΔV decreases monotonically to $\Delta V \approx 0.32$ V, indicating that the dipole moment of the second layer is, on average, antiparallel to that of the first layer. Last, when the third layer starts to form, the surface potential exhibits a 6 mV step only. Harke et al. have reported similar observations,²⁶ except that in their case the second layer nucleating on top of the first one is actually a bilayer, at least partially.

We may estimate the out-of-plane dipole moment μ_{\perp} of our Langmuir film by means of the Helmholtz equation $\mu_{\perp} = \epsilon_r \epsilon_0 A \Delta V$, where ϵ_r and ϵ_0 are the relative and vacuum dielectric permittivities and A is the molecular area at which a ΔV jump of surface potential has occurred.²⁷ The main limitation^{28–30} to the use of this equation in such a case arises from the facts that the monolayer is not electrically uniform, because ϵ_r varies along the molecular axis, and that ϵ_r is not precisely known for all chemical species. Assuming²¹ a value of $\epsilon_r \approx 3$ yields a maximum normal moment $\mu_{\max} \approx 3.5 \text{ D}$ when $A \approx 113 \text{ \AA}^2$. Regardless of the aforementioned limitations, the dipole moment is proportional to the product $A\Delta V$, which is plotted against the molecular area in the inset to Figure 2. It can be seen that the moment is maximum at point A, that is, when the molecules get closer and the surface pressure takes off. The anchoring of molecules at the air–water interface can lead to a significant decrease of their total dipole moment because of the screening effect of water. We believe that this is not the case here and that even on water the total dipole moment of our molecule must be close to 5.9 D because the anchoring at the interface is assumed to be made through the siloxane part and therefore no screening of the two major dipoles can occur. Hence, if we take the measured normal value of 3.5 D as correct, we estimate the dipole moment to be at an angle of $\cos^{-1}(3.5/5.9) \approx 54^\circ$ with the normal to the surface. Consequently, since the dipole is oriented at 28° to the cores, the molecules make an angle of ca. 82° to the normal, that is, lie almost flat on the water at point A. Though very crude, these calculations give a result in good agreement with the tilt angle of 79° obtained from the isotherm, so we can at least draw the a minima conclusion that the molecules of the first layer are very tilted. The component of the polarization (per volume unit) normal to the surface P_{\perp} can also be estimated since $P_{\perp} = \mu_{\perp}/Ad$, where d is the thickness of the film and Ad is the molecular volume. We find $P_{\perp} \approx 550 \text{ nC}\cdot\text{cm}^{-2}$, which is 3 times more than the transverse polarization measured in the bulk SmC* phase.¹⁵

To get more information on the structure, Langmuir–Blodgett films of mono- and bilayers have been transferred on hydrophilic substrates and studied with X-ray reflectivity. Transfers performed at a surface pressure of $10 \text{ mN}\cdot\text{m}^{-1}$ (monolayer regime) and $15.5 \text{ mN}\cdot\text{m}^{-1}$ (bilayer regime) have a transfer ratio of ~ 1.5 , meaning that important molecular rearrangements take place. It is therefore not possible to directly transpose their thickness to that of the Langmuir films on water, but the measurements

still have an indicative value. The monolayer LB films have a thickness of $17 \pm 1 \text{ \AA}$ and are analyzed easily. Bilayer films have been analyzed as such, on modeling the electronic densities of the various chemical groups (siloxanes, phenyl, etc.).³¹ We have considered each layer as being made of three blocks: siloxane + C_6 chain, core (benzene rings), and sulfinate + C_{10} chain. Each block is characterized by two parameters, electronic density³² and thickness. For all sublayers we have considered the roughness constant and equal to 4 \AA , as freeing this parameter did not change much the fit. This was also done with the purpose of keeping the number of parameters as low as possible, which is to be done if somewhat realistic values have to be extracted from the fit. The fit is reasonably good, as seen in Figure 3, with the result that the bottom layer is $20.3 \pm 0.5 \text{ \AA}$ thick and the top one is $31.0 \pm 0.5 \text{ \AA}$. The inset in Figure 3 gives the variation of δ as a function of the distance to the silicon substrate. The conclusion that can be drawn from the analysis of the X-ray spectrum is that the LB film is actually bilayered, that the molecules are not oriented in the same direction within the two layers, and that the molecules are closer to the vertical in the upper layer ($\sim 49^\circ$) and very tilted ($\sim 64^\circ$) in the bottom layer. In both layers the molecules are therefore more tilted in the LB film than in the bulk SmC* phase.

Brewster angle microscopy (see sketch in Figure 6) is based on the fact that, at the Brewster angle, the light that is polarized in the plane of incidence is not reflected at an air–water interface. If a film of material having an index of refraction different from that of water is present at the surface, Brewster conditions are not fulfilled any longer and some light is reflected, allowing for an image of the film to be recorded. Figure 4 shows such BAM pictures of our Langmuir film at different stages of its compression isotherm. For all pictures the polarizer and analyzer of the microscope are set parallel to the plane of incidence. The film is initially in a liquid condensed phase, with the molecules forming structures with curved smooth boundaries (Figure 4a) and the holes in the film closing nicely upon compression giving a perfect monolayer (Figure 4b). At point B, the nucleation of the second layer is conspicuous with the occurrence of brighter dots (Figure 4c). If the compression is pursued, the dots grow as disks, looking inhomogeneous with shadowing structures inside (Figure 4d) that look very much like the nematic phase of a liquid crystal under a polarizing microscope (Schlieren textures). The Brownian motion is very sensible, as each time a strongly tilted sample is observed in polarized light, due to the excellent coupling of light with the director in this configuration. After a little waiting time, the inner structure of the disks forms rings and spirals with alternating black and white domains (Figure 4e,f). The observation being performed in polarized light, these patterns correspond to domains where the main molecular axis is parallel or perpendicular to the polarization of the light. When the film is further compressed, the different disks merge and eventually, at point C on the isotherm, the whole surface is covered with these Schlieren textures (Figure 4g). Last, the emergence of a third layer can be seen at the end of the compression, as more disks with similar substructures form (Figure 4h). Upon decompression, as mentioned above, things go back in reverse order layer after layer, with holes forming and expanding, resulting in two-dimensional foams clearly seen in the last pictures (Figure 4i,j). The observed behavior, as described, showed no dependence on temperature within the $10\text{--}30^\circ\text{C}$ range.

Such nematic-like patterns are rather unusual in Langmuir films,^{22,33–35} but they have been obtained more frequently in

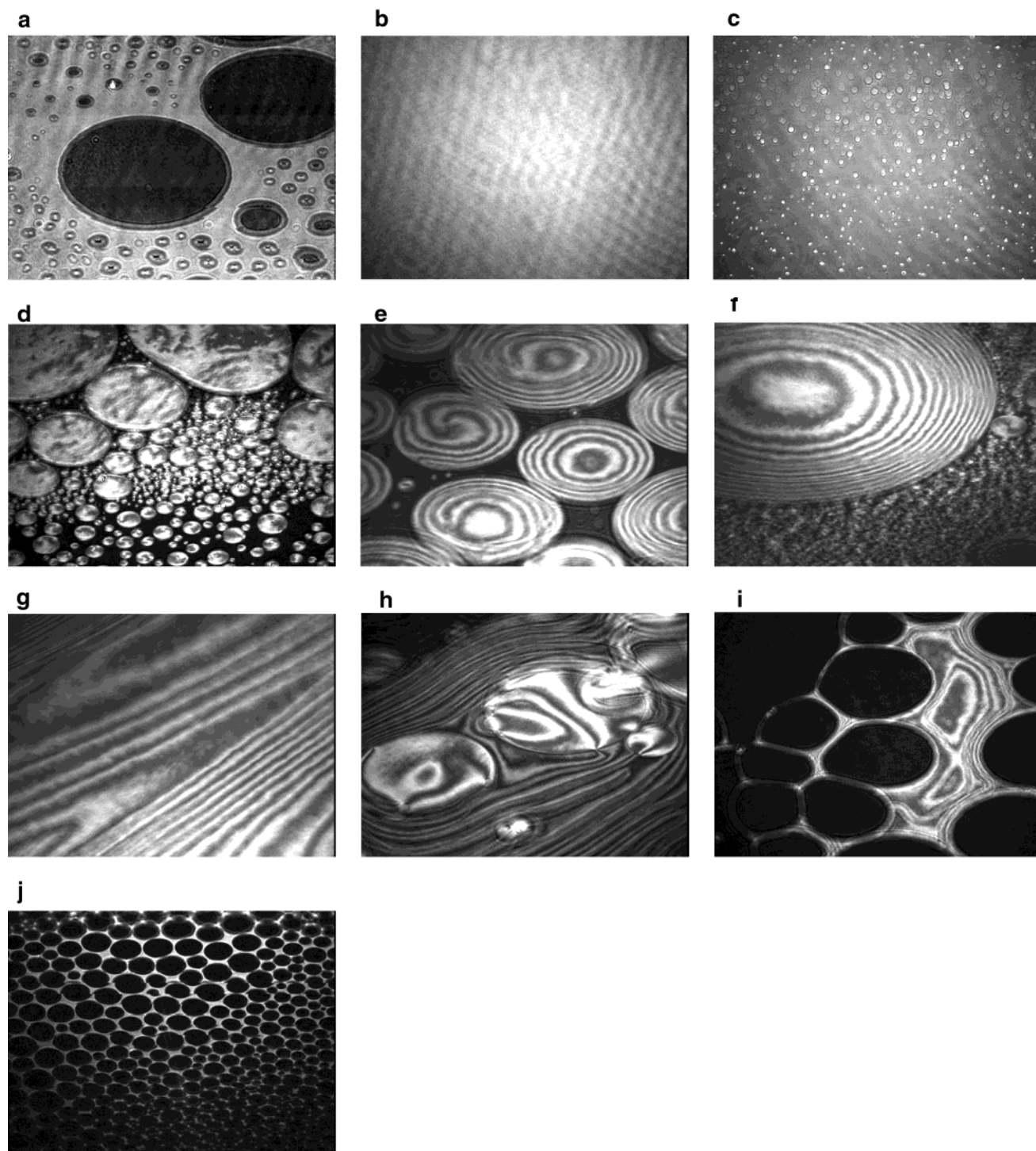


Figure 4. (a) BAM picture of the Langmuir film on water at molecular area $A = 330 \text{ \AA}^2$. Round black disks are holes in the film through which water can be seen. (b) BAM picture of the Langmuir film on water at molecular area $A = 115 \text{ \AA}^2$. The first layer is complete and homogeneous. (c) BAM picture of the Langmuir film on water at molecular area $A = 110 \text{ \AA}^2$. The second layer is nucleating (little white dots) on top of the first one. (d) BAM picture of the Langmuir film on water at molecular area $A = 50 \text{ \AA}^2$. Upon further compression the second layer grows larger with visible substructures within the disks. (e) BAM picture of the Langmuir film on water at molecular area $A = 35 \text{ \AA}^2$ (slightly before point C). After a few minutes, the structures in the disks form either concentric or spiraling lines. (f) BAM picture of the Langmuir film on water at molecular area $A = 35 \text{ \AA}^2$ after a waiting time of 5 min. The disks grow larger and the substructures finer. (g) BAM picture of the Langmuir film on water at molecular area $A = 35 \text{ \AA}^2$ after a waiting time of 35 min. The second layer eventually fills the field of view; the disks are not visible any longer. (h) BAM picture of the Langmuir film on water at molecular area $A = 14 \text{ \AA}^2$. The third layer (brighter structures) can be seen nucleating on top of the second layer (blurred lines). (i) BAM picture of the Langmuir film on water at molecular area $A = 83 \text{ \AA}^2$ during decompression. (j) BAM picture of the Langmuir film on water at molecular area $A = 200 \text{ \AA}^2$ during decompression.

surface-induced films,¹⁰ free-standing films (though with artificial means in this case^{36–38}), and hybrid films.¹¹ Tabe et al. describe similar looking Schlieren textures in a Langmuir film obtained with a smectic C compound. Their experimental setup

was different,³⁴ essentially in the much smaller ($\sim 17^\circ$) incidence angle.³⁹ The experiment of Ibn-Elhaj et al. has some resemblance with ours in that their molecules possess a siloxane moiety, with a strong axial dipolar moment, and that they form multilayered

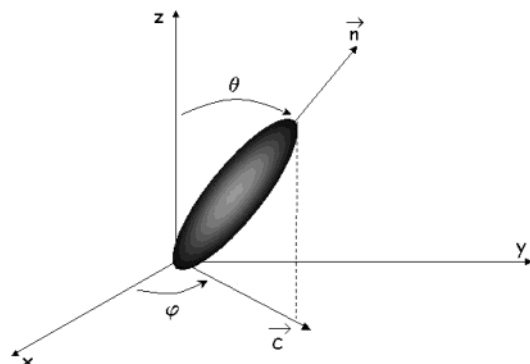


Figure 5. Diagram defining the vectors and angles.

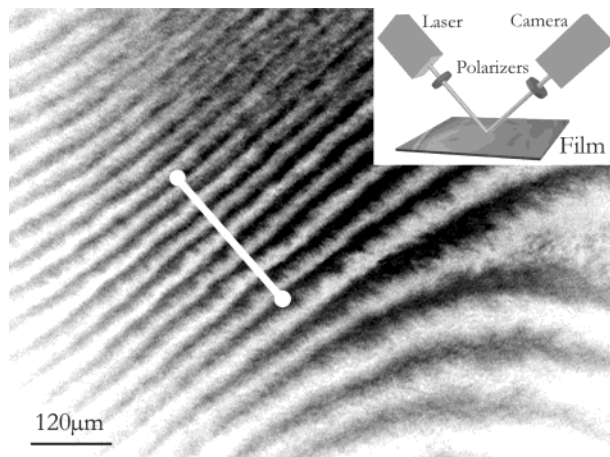


Figure 6. BAM picture of the film with indication of the line scan. The contrast is poorer at the edges of the picture because of the limited depth of field (see Experimental Section). Inset is a schematic diagram of the imaging setup. The axes of both polarizers are within the plane of incidence.

films on the Langmuir trough. Nevertheless, they observe Schlieren textures with Brewster angle microscopy in the first layer and an isotropic phase in subsequent ones, while on the contrary we observe an isotropic first layer and birefringent second and third layers. The difference in behavior probably can probably be ascribed to the relative position of the siloxane chain and the chiral sulfinate group.

A more detailed analysis of the fringes and structures will be given elsewhere, but our observations can already be discussed qualitatively. If one defines a vector \vec{c} as the in-plane projection of the molecular long axis (Figure 5), the alternating black and white fringes that can be seen in the BAM pictures correspond to the periodic variation of \vec{c} turning periodically within the plane (see sketch in Figure 7). When \vec{c} is perpendicular to the plane of incidence, the domain appears black; when \vec{c} is in the plane of incidence (i.e., parallel to the polarizers), the domain looks white with an intensity that depends on the molecular orientation relative to the incident beam. A linear scan taken along a line perpendicular to the fringes (Figure 6) gives the video intensity as a function of position, plotted in Figure 7. It exhibits continuous variations which indicate that the distortion contains no defects—such as disclination lines—as often observed in similar patterns, with minima and two different types of maxima. The intensity of the reflected light is maximum when the molecules are within the plane of incidence, but as they rotate, they can be tilted toward either the direction of the laser or that of the camera (see sketch in Figure 6). The reflected intensity is higher in the former case than in the latter. The effect is clearly seen in Figure

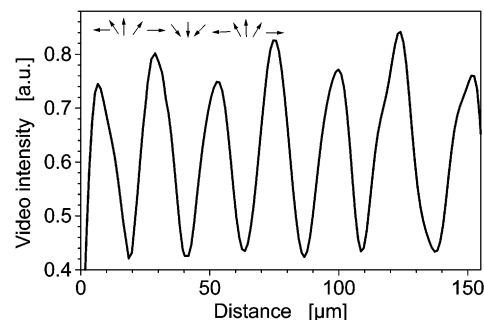


Figure 7. Video intensity as a function of position along the line scan of Figure 6. The noise level has been reduced by averaging five parallel scans. The little arrows represent the orientation of \vec{c} within the film, along the scan line.

7, with the intensity of every second maximum being larger. The distortion is therefore analogous to the one discussed in surface-induced films;^{9,10} it corresponds similarly to a continuous rotation of the director. More significantly, it also appears spontaneously, which indicates that the energy of the distorted film is surprisingly lower than that of the uniform state. The symmetry of both systems is moreover the same: the film is sandwiched between two different media (asymmetric boundaries) and its molecules are tilted. All these common features allow one to infer that the mechanism that governs the formation of the structures presented here is essentially the same as the one discussed in ref 9. We therefore propose that the observed distortion is an effect of surface elasticity that favors a particular splay distortion, positive or negative, associated with a slight tilt modulation. When the associated surface elastic constant K_1 (as defined in ref 9) reaches a threshold value, the continuous distortion of \vec{c} becomes energetically favorable. In other words and in a very simplified way, one may say that the molecules have some natural tendency not to stay parallel to each other but rather to slightly diverge. A simple reason for that could be the difference in cross section between the rigid core and the siloxane moieties of the molecule. The force behind the observed precession of \vec{c} in Langmuir films consequently stems from the fact that the molecules are forced into a common orientation when they would rather flip. They cannot do so because of their van der Waals interactions with the underlying layer (the microphase separation between alkanes and siloxanes). The phenomenon is not observed in the first layer (no optical structures) where the molecules can rotate almost freely, and where, therefore, no \vec{c} director exists.

The antiparallel pairing of the overlapping molecules forming the second “layer” in ref 22 forbids the observation of Schlieren textures as the effective K_1 constant of such a dimer is much smaller than that of single molecules: dimers can stay parallel to each other and perpendicular to the layer plane at minimal energy cost. For this reason the BAM pictures only show isotropic islands with no birefringence.

Last, let us emphasize that the structure of the first layer (the one directly in contact with water) is very probably altered whenever the film becomes bilayered. There is no direct experimental evidence supporting this assertion: with our imaging setup, the light which contributes to the BAM pictures is reflected from the entire film (at least as long as the film thickness is less than the light wavelength), and it is therefore impossible to selectively observe what is underneath the uppermost layer. Still, it is hard to imagine that the upper layer could develop some degree of organization without the bottom layer doing so: it is well-known that in smectics or cholesterics

the position and orientation of the molecules in adjacent layers are interdependent.

IV. Conclusion

A mesogenic molecule having a SmC* phase in the bulk has been studied at the air–water interface and shown to produce Langmuir films with particularly reversible isotherms. It seems interesting to test other molecules also having a siloxane group attached to a rigid core to check if their isotherms similarly exhibit such an exceptional reversibility. Surface pressure measurements and Brewster angle microscopy show that the compound easily forms multilayered films, which are stable enough to be transferred as such on solid substrates. Due to the low symmetry of the system, the Langmuir film has a surface elasticity that appears to be strong enough to promote a spontaneous distortion in the second and third layers of the film. Unusual textures with periodic disclination lines are then observed with Brewster angle microscopy. These textures are the evidence of the continuous rotation of the in-plane projection of the molecular long axis. A detailed analysis of these textures will be the subject of a subsequent paper.

Acknowledgment. Financial support from NEDO (“New dipolar liquid-crystals”, Contract No. 98MB1) is gratefully acknowledged. It is our pleasure to thank the people at NFT, especially Dr. D. Hoenig, for their constant and efficient support.

References and Notes

- (1) Glaser, R.; Kaszynski, P. *Anisotropic organic materials—Approaches to polar order*; American Chemical Society: Washington, DC, 2001; Vol. 798.
- (2) Holman, K. T.; Pivovar, A. M.; Ward, M. D. *Science* **2001**, 294, 1907.
- (3) Guillon, D. *Adv. Liq. Cryst.* **2000**, 113, 1.
- (4) Meyer, R. B.; Liebert, L.; Strzelecki, L.; Keller, P. *J. Phys. Lett. (Paris)* **1975**, 36, 69.
- (5) Lubensky, T. C. *Science* **2000**, 288, 2146.
- (6) Lagerwall, S. T. *Ferroelectric and antiferroelectric liquid crystals*; Wiley-VCH: Weinheim, 1999.
- (7) Young, C. Y.; Pindak, R.; Clark, N. A.; Meyer, R. B. *Phys. Rev. Lett.* **1978**, 40, 773.
- (8) Galerne, Y. *Europhys. Lett.* **1992**, 18, 511.
- (9) Najjar, R.; Galerne, Y. *Mol. Cryst. Liq. Cryst.* **1999**, 328, 489.
- (10) Najjar, R.; Galerne, Y. *Europhys. Lett.* **2001**, 55, 355.
- (11) Link, D. R.; Nakata, M.; Takanishi, Y.; Ishikawa, K.; Takezoe, H. *Phys. Rev. Lett.* **2001**, 87, 1955071.
- (12) Ulman, A. *Ultrathin organic films*; Academic Press Inc.: New York, 1991.
- (13) 1 debye (D) = 3.33×10^{-10} C·m.
- (14) Guillon, D.; Osipov, M. A.; Méry, S.; Siffert, M.; Nicoud, J. F.; Bourgogne, C.; Sebastião, P. *J. Mater. Chem.* **2001**, 11, 2700.
- (15) Sebastião, P.; Méry, S.; Siffert, M.; Nicoud, J. F.; Galerne, Y.; Guillon, D. *Ferroelectrics* **1998**, 212, 133.
- (16) Cherkaoui, M. Z.; Nicoud, J. F.; Galerne, Y.; Guillon, D. *J. Chem. Phys.* **1997**, 106, 7816.
- (17) Hénon, S.; Meunier, J. *Rev. Sci. Instrum.* **1991**, 62, 936.
- (18) Lheveder, C.; Hénon, S.; Mercier, R.; Tissot, G.; Fournet, P.; Meunier, J. *Rev. Sci. Instrum.* **1998**, 69, 1446.
- (19) Israelachvili, J. *Intermolecular and surface forces*; Academic Press: San Diego, 1992.
- (20) Shapovalov, V. L. *Thin Solid Films* **1998**, 327–329, 816.
- (21) Ibn-Elhaj, M.; Cherkaoui, M. Z.; Zniber, R.; Möhwald, H. *J. Phys. Chem. B* **1998**, 102, 5274.
- (22) Ibn-Elhaj, M.; Riegler, H.; Möhwald, H. *J. Phys. I (Fr.)* **1996**, 6, 969.
- (23) The molecules studied in the publication of Ibn-Elhaj are based on a cyano-biphenyl core which produces so-called “bilayered smectics”, in which each smectic layer is made of interdigitated antiparallel molecules (SmA_d).
- (24) Zhang, T.; Feng, Z.; Wong, G. W.; Ketterson, J. B. *Langmuir* **1996**, 12, 2298.
- (25) Rapp, B.; Gruler, H. *Phys. Rev. A* **1990**, 42, 2215.
- (26) Harke, M.; Ibn-Elhaj, M.; Möhwald, H.; Motschmann, H. *Phys. Rev. E* **1998**, 57, 1806.
- (27) Novais de Oliveira, O. J.; Taylor, D. M.; Lewis, T. J.; Salvagno, S.; Stirling, C. J. M. *J. Chem. Soc., Faraday Trans. 1* **1989**, 85, 1009.
- (28) Vogel, V.; Möbius, D. *J. Colloid Interface Sci.* **1988**, 126, 408.
- (29) Demchak, R. J.; Fort, T. J. *J. Colloid Interface Sci.* **1974**, 46, 191.
- (30) Taylor, D. M.; Novais de Oliveira, O. J.; Morgan, H. *J. Colloid Interface Sci.* **1990**, 139, 508.
- (31) Als-Nielsen, J.; McMorrow, D. *Elements of modern X-ray physics*; John Wiley & Sons: New York, 2001.
- (32) Strictly speaking, δ is not the electronic density but is directly proportional to it (see ref 31, Chapter 3).
- (33) Adams, J.; Rettig, W.; Duran, R. S.; Naciri, J.; Shashidar, R. *J. Phys. Chem.* **1993**, 97, 2021.
- (34) Tabe, Y.; Shen, N.; Mazur, E.; Yokoyama, H. *Phys. Rev. Lett.* **1999**, 82, 759.
- (35) Tabe, Y.; Yokoyama, H. *J. Chem. Phys.* **2001**, 115, 1041.
- (36) Cladis, P. E.; Couder, Y.; Brand, H. R. *Phys. Rev. Lett.* **1985**, 55, 2945.
- (37) Link, D. R.; Radzihovsky, L.; Natale, G.; MacLennan, J. E.; Clark, N. A. *Phys. Rev. Lett.* **2000**, 84, 5772.
- (38) Najjar, R.; Galerne, Y. *Mol. Cryst. Liq. Cryst.* **2001**, 366, 421.
- (39) This setup called depolarized reflected light microscope (DRLM) has been described by Pindak et al.⁴⁰ The main advantage is that the focus is sharp over the entire field of view, the drawback being that only birefringent films can be imaged.
- (40) Pindak, R.; Young, C. Y.; Meyer, R. B.; Clark, N. A. *Phys. Rev. Lett.* **1980**, 45, 1193.